Low-density instabilities in relativistic asymmetric matter of compact stars

C. Providência and L. Brito
Centro de Física Teórica, Departamento de Física, Universidade de Coimbra, P-3004-516 Coimbra, Portugal

S. S. Avancini[1] and D. P. Menezes[1,2]
[1]*Depto de Física, CFM, Universidade Federal de Santa Catarina, Florianópolis, SC, CP. 476, CEP 88.040-900, Brazil*
[2]*School of Physics, University of Sydney, New South Wales 2006, Australia*

Ph. Chomaz
GANIL (DSM-CEA/IN2P3-CNRS), B.P. 5027, F-14076 Caen Cédex 5, France
(Received 2 August 2005; published 16 February 2006)

Dynamical instability modes of low-density asymmetric nuclear matter (ANM) neutralized by electrons as found in supernova core and neutron star crust are studied in the framework of relativistic mean-field hadron models with the inclusion of electron and photon fields. The dynamical and thermodynamical instability zones are compared. It is shown that the Coulomb field quenches large structure formation but has little effect on medium and small-size fluctuations that are, however, partially stabilized by the finite range of the nuclear forces. The electron dynamics tends to restore the large-wavelength instabilities but is moderated by the high-electron Fermi energy.

DOI: 10.1103/PhysRevC.73.025805 PACS number(s): 21.60.Ev, 21.65.+f, 24.10.Jv, 71.10.Ay

I. INTRODUCTION

The understanding of compact stars, supernova cores, and neutron stars requires a multidisciplinary theoretical effort, including astrophysics, nuclear and particle physics, and thermodynamics. Stellar matter at low density is essentially composed of neutrons, protons, electrons, and, possibly, when their mean free path is short enough, neutrinos. This composite matter is expected to undergo phase transitions associated to the nuclear liquid-gas phase transition but strongly modified by the Coulomb interaction and the presence of electrons [1–14]. Those phase transitions may affect the mechanical, thermal, and transport properties of compact stars. An important characteristic of the nuclear liquid-gas phase transition is the role of isospin. Indeed, because nuclear matter is composed of two different fluids, namely protons and neutrons, the liquid gas phase transition can lead to an isospin distillation phenomenon.

The role of isospin has been first discussed in the context of nuclear matter phase transition in connection with the fragmentation of hot nuclei. In Ref. [15], based on a lattice-gas model, the authors have shown that the distillation effect indeed influences the light fragment production. In Ref. [16] it was shown that for a neutron-rich system undergoing a phase transition, the fraction of light neutron rich isotopes (such as tritium) compared with neutron poor ones (such as ^{3}He) is much larger than what would be expected looking only at the isospin asymmetry (N/Z) of the source. This strong enhancement of light neutron-rich particles has been interpreted as a signature of the fractionation effect [16]. Hence, instabilities and phase transitions of asymmetric nuclear matter (ANM) are important quantities in the understanding of the physics underlying isospin distillation and multifragmentation.

At low nuclear densities, mechanical and chemical modes are coupled in such a way that the instability of the ANM system appears as a unique mode being a mixture of baryon density and concentration fluctuations [17]. The region of instability, determined by the spinodal curve, depends on the relativistic model used and on its parametrization and shrinks considerably with the increase of the temperature [18] within a mean-field approximation. Including finite size effects and the Coulomb interaction within a Thomas-Fermi finite temperature approach [19] reduces drastically the critical temperature.

To describe compact-star matter, the electrons must be introduced. They neutralize the proton charge and thus suppress the diverging Coulomb contribution to the energy. In such a context, the Coulomb interaction is only sensitive to the charge correlation. Calculations going beyond mean-field and including correlations seem to indicate that, in compact-star matter the critical temperature will increase because of the larger energy gap between a pure phase and mixed phase [20]. Not only the equation of state of stellar matter has to be understood, but also the neutrino mean free path in the medium has to be well described. It has been shown that the neutrino opacity is affected by nucleon-nucleon interactions because of coherent scattering off density fluctuations [21]. Both single particle and collective contribution have to be taken into account. It is, therefore, important to have a through out understanding of the collective modes in asymmetric nuclear matter to predict the behavior of neutrinos.

In a previous work [22] we have studied the longitudinal nuclear and mesonic collective modes arising from small oscillations around a stationary state in nuclear matter. This investigation was performed in the framework of a relativistic mean-field hadronic model within the Vlasov formalism. In the present work we investigate the influence of the electromagnetic interaction and of the presence of electrons on the unstable modes and compare the dynamical instability region with the thermodynamical one. We study in some details the role of isospin and the modification of the distillation phenomenon because of the presence of the Coulomb field and electrons.

Relativistic phenomenological models have been extensively used in the description of nuclear and stellar properties. For densities up to nuclear saturation density they predict similar results for the equation of state of nuclear matter and ground-state properties of nuclei. However, differences may occur at large densities and/or finite temperatures. They should, therefore, be tested on a larger interval of densities and temperatures to have predictive power.

In Sec. II we formulate the Vlasov equation formalism for nuclear neutral matter, including electrons and the electromagnetic field. In Sec. III the dispersion relation is displayed and in Sec. IV a brief review of the thermodynamical unstable region is given. In Sec. V the numerical results are shown and discussed. Finally, in the last section the most important conclusions are drawn.

II. THE VLASOV EQUATION FORMALISM

We consider a system of baryons, with mass M interacting with and through an isoscalar-scalar field ϕ with mass m_s, an isoscalar-vector field V^μ with mass m_v, and an isovector-vector field $\mathbf{b}^\mu$ with mass m_ρ. We also include a system of electrons with mass m_e. Protons and electrons interact through the electromagnetic field A^μ. The Lagrangian density reads as follows:

$$\begin{aligned}\mathcal{L} = \bar{\psi}\left[\gamma_\mu\left(i\partial^\mu - g_v V^\mu - \frac{g_\rho}{2}\boldsymbol{\tau}\cdot\mathbf{b}^\mu - eA^\mu\frac{1+\tau_3}{2}\right) - (M - g_s\phi)\right]\psi \\ + \frac{1}{2}\left(\partial_\mu\phi\partial^\mu\phi - m_s^2\phi^2\right) - \frac{1}{3!}\kappa\phi^3 - \frac{1}{4!}\lambda\phi^4 \\ - \frac{1}{4}\Omega_{\mu\nu}\Omega^{\mu\nu} + \frac{1}{2}m_v^2 V_\mu V^\mu - \frac{1}{4}\mathbf{B}_{\mu\nu}\cdot\mathbf{B}^{\mu\nu} + \frac{1}{2}m_\rho^2\mathbf{b}_\mu\cdot\mathbf{b}^\mu \\ - \frac{1}{4}F_{\mu\nu}F^{\mu\nu} + \bar{\psi}_e[\gamma_\mu(i\partial^\mu + eA^\mu) - m_e]\psi_e, \qquad (1)\end{aligned}$$

where $\Omega_{\mu\nu} = \partial_\mu V_\nu - \partial_\nu V_\mu$, $\mathbf{B}_{\mu\nu} = \partial_\mu\mathbf{b}_\nu - \partial_\nu\mathbf{b}_\mu - g_\rho(\mathbf{b}_\mu\times\mathbf{b}_\nu)$, and $F_{\mu\nu} = \partial_\mu A_\nu - \partial_\nu A_\mu$. The model comprises the following parameters: Three coupling constants g_s, g_v, and g_ρ of the mesons to the nucleons, the nucleon mass M, the electron mass m_e, the masses of the mesons m_s, m_v, m_ρ, the electromagnetic coupling constant $e = \sqrt{4\pi/137}$, and the self-interacting coupling constants κ and λ. We have used the set of constants identified as NL3 taken from Ref. [23]. For this case, the saturation density that we refer as ρ_0 is 0.148 fm^{-3}.

We denote by $f(\mathbf{r},\mathbf{p},t) = \mathrm{diag}(f_p, f_n, f_e)$ the one-body phase-space distribution function in isospin space and by

$$h = \begin{pmatrix} \sqrt{(\mathbf{p}-\boldsymbol{\mathcal{V}}_p)^2 + (M-g_s\phi)^2} + \mathcal{V}_{0p} & 0 & 0 \\ 0 & \sqrt{(\mathbf{p}-\boldsymbol{\mathcal{V}}_n)^2 + (M-g_s\phi)^2} + \mathcal{V}_{0n} & 0 \\ 0 & 0 & \sqrt{(\mathbf{p}+e\mathbf{A})^2 + m_e^2} - eA_0 \end{pmatrix} \qquad (2)$$

the one-body Hamiltonian, where

$$\begin{aligned}\mathcal{V}_{0i} &= g_v V_0 + \frac{g_\rho}{2}\tau_i b_0 + eA_0\frac{1+\tau_i}{2}, \\ \boldsymbol{\mathcal{V}}_i &= g_v\mathbf{V} + \frac{g_\rho}{2}\tau_i\mathbf{b} + e\mathbf{A}\frac{1+\tau_i}{2}, \qquad i = p, n\end{aligned}$$

$\tau_i = 1$ (protons) or -1 (neutrons).

The time evolution of the distribution function is described by the Vlasov equation

$$\frac{\partial f_i}{\partial t} + \{f_i, h_i\} = 0, \qquad i = p,\ n,\ e, \qquad (3)$$

where $\{,\}$ denotes the Poisson brackets. It has been argued in Refs. [24,25] that Eq. (3) expresses the conservation of the number of particles in phase space and is, therefore, covariant. Antiparticles should certainly be taken into account at finite temperature. However, at a given temperature, the dynamics described by the Vlasov equation do not change the number of particles or antiparticles in this semiclassical approach. From Hamilton's equations we derive the equations describing the time evolution of the fields ϕ, V^μ, A^μ and the third component of the ρ field $b_3^\mu = (b_0, \mathbf{b})$ [22].

At zero temperature and for particles obeying Fermi-Dirac statistics, the value of the distribution function is either 1 or 0, because the single-particle state is either occupied by one particle or empty. The state that minimizes the energy of asymmetric nuclear matter is characterized by the Fermi momenta $P_{Fi}, i = p, n$, $P_{Fe} = P_{Fp}$ and is described by the distribution function

$$f_0(\mathbf{r},\mathbf{p}) = \mathrm{diag}\left[\Theta\left(P_{Fp}^2 - p^2\right), \Theta\left(P_{Fn}^2 - p^2\right), \Theta\left(P_{Fe}^2 - p^2\right)\right] \qquad (4)$$

and by the constant mesonic fields that obey the following equations: $m_s^2\phi_0 + \frac{\kappa}{2}\phi_0^2 + \frac{\lambda}{6}\phi_0^3 = g_s\rho_s^{(0)}$, $m_v^2 V_0^{(0)} = g_v j_0^{(0)}$, $V_i^{(0)} = 0$, $m_\rho^2 b_0^{(0)} = \frac{g_\rho}{2} j_{3,0}^{(0)}$, $b_i^{(0)} = 0$, $A_0^{(0)} = 0$, and $A_i^{(0)} = 0$.

Collective modes in the present approach correspond to small oscillations around the equilibrium state, and they are described by the linearized equations of motion. We take for the fields

$$\begin{aligned} f &= f_0 + \delta f, \quad & \phi &= \phi_0 + \delta\phi, \quad & V_0 &= V_0^{(0)} + \delta V_0, \\ V_i &= \delta V_i, & b_0 &= b_0^{(0)} + \delta b_0, & b_i &= \delta b_i, \\ A_0 &= \delta A_0, & A_i &= \delta A_i. \end{aligned} \qquad (5)$$

As in Ref. [26] we introduce a generating function $S(\mathbf{r},\mathbf{p},t) = \mathrm{diag}\left(S_p, S_n, S_e\right)$, defined in isospin space such that the variation of the distribution function is

$$\delta f_i = \{S_i, f_{0i}\} = -\{S_i, p^2\}\delta\left(P_{Fi}^2 - p^2\right). \qquad (6)$$

In terms of this generating function, the linearized Vlasov equations for δf_i are equivalent to the following time evolution

equations

$$\frac{\partial S_e}{\partial t} + \{S_e, h_{0e}\} = \delta h_e = -e\left[\delta A_0 - \frac{\mathbf{p}\cdot\delta\mathbf{A}}{\epsilon_{0e}}\right], \quad (7)$$

$$\frac{\partial S_i}{\partial t} + \{S_i, h_{0i}\} = \delta h_i = -g_s\delta\phi\frac{M^*}{\epsilon_0} + \delta\mathcal{V}_{0i} - \frac{\mathbf{p}\cdot\delta\boldsymbol{\mathcal{V}}_i}{\epsilon_0}, \quad i = p, n, \quad (8)$$

where $\delta\mathcal{V}_{0i} = g_v\delta V_0 + \tau_i\frac{g_\rho}{2}\delta b_0 + e\frac{1+\tau_i}{2}\delta A_0$ and $\delta\boldsymbol{\mathcal{V}}_i = g_v\delta\mathbf{V} + \tau_i\frac{g_\rho}{2}\delta\mathbf{b} + e\frac{1+\tau_i}{2}\delta\mathbf{A}$, which has to be satisfied only for $p = P_{Fi}$. In Eq. (7) $\epsilon_{0e} = \sqrt{p^2 + m_e^2}$ and in Eq. (8)

$$h_{0i} = \sqrt{p^2 + M^{*2}} + \mathcal{V}_{0i}^{(0)} = \epsilon_0 + \mathcal{V}_{0i}^{(0)}. \quad (9)$$

The linearized equations of the fields are obtained using the procedure already presented in Ref. [22]. The longitudinal modes, with momentum $\mathbf{k}$ and frequency ω are well described by the ansatz

$$\begin{pmatrix} S_j(\mathbf{r},\mathbf{p},t) \\ \delta\phi \\ \delta B_0 \\ \delta B_i \end{pmatrix} = \begin{pmatrix} \mathcal{S}_\omega^j(\cos\theta) \\ \delta\phi_\omega \\ \delta B_\omega^0 \\ \delta B_\omega^i \end{pmatrix} e^{i(\omega t - \mathbf{k}\cdot\mathbf{r})},$$

where $j = e, p, n$, $B = V, b, A$ represents the vector-meson fields and θ is the angle between $\mathbf{p}$ and $\mathbf{k}$. For these modes, we get $\delta V_\omega^x = \delta V_\omega^y = 0$, $\delta b_\omega^x = \delta b_\omega^y = 0$, and $\delta A_\omega^x = \delta A_\omega^y = 0$.

It is worth pointing out that the present formalism was first applied to determine the collective modes in symmetric nuclear matter at both zero and finite temperature in Ref. [26], where it was shown that the Landau-Vlasov formalism was equivalent to the Green function formalism developed in Ref. [27], giving similar results. In Ref. [28], the formalism of Refs. [27] and [29] was extended to asymmetric hadronic matter. In the last article the inclusion of electrons was also considered. These two articles deal with neutrino interaction in hot dense uniform hadronic matter, including electromagnetic interaction. However, the low-density inhomogeneous matter, which is the main point of our article, has not been discussed.

III. DISPERSION RELATION

Equations (7) and (8) are written in terms of the amplitudes $A_{\omega i}$ related to the transition densities by

$$\delta\rho_i = \frac{3}{2}\frac{k}{P_{Fi}}\rho_{0i}A_{\omega i}. \quad (10)$$

We get

$$\begin{bmatrix} 1 - \left(-C_s^{pp} + C_v^{pp} + C_\rho^{pp} + C_A^{pp}\right)L(s_p) & \left(C_s^{pn} - C_v^{pn} + C_\rho^{pn}\right)L(s_p) & C_A^{pe}L(s_p) \\ \left(C_s^{np} - C_v^{np} + C_\rho^{np}\right)L(s_n) & 1 - \left(-C_s^{nn} + C_v^{nn} + C_\rho^{nn}\right)L(s_n) & 0 \\ C_A^{ep}L(s_e) & 0 & 1 - C_A^{ee}L(s_e) \end{bmatrix} \begin{pmatrix} A_{\omega p} \\ A_{\omega n} \\ A_{\omega e} \end{pmatrix} = 0, \quad (11)$$

with $A_{\omega i} = \int_{-1}^{1} x S_{\omega i}(x)dx$ and $L(s_i)$ related to the Lindhard function Φ by

$$L(s_i) = 2\Phi(s_i) = 2 - s_i\ln\left(\frac{s_i+1}{s_i-1}\right), \quad (12)$$

with $s_i = \omega/\omega_{oi} = \omega/(kV_{Fi})$, $V_{F_i} = P_{F_i}/\epsilon_{F_i}$ being the Fermi velocity of particle i. We also have

$$C_s^{ij} = \frac{1}{2\pi^2}\frac{M^{*2}g_s^2}{\omega^2 - \omega_s^2}\frac{1}{P_{Fi}}P_{Fj}V_{Fj},$$

$$C_v^{ij} = \frac{1}{2\pi^2}\frac{g_v^2}{\omega^2 - \omega_v^2}\left(1 - \frac{\omega^2}{k^2}\right)\frac{P_{Fj}^2}{V_{Fi}},$$

$$C_\rho^{ij} = \frac{1}{2\pi^2}\frac{g_\rho^2}{4\left(\omega^2 - \omega_\rho^2\right)}\left(1 - \frac{\omega^2}{k^2}\right)\frac{P_{Fj}^2}{V_{Fi}},$$

$$C_A^{ij} = -\frac{e^2}{2\pi^2}\frac{1}{k^2}\frac{P_{Fj}^2}{V_{Fi}},$$

where $\epsilon_{Fi} = \sqrt{P_{Fi}^2 + M^{*2}}$, $i = p, n$ and $\omega_s^2 = k^2 + m_{s,\text{eff}}^2$, $\omega_v^2 = k^2 + m_v^2$, $\omega_\rho^2 = k^2 + m_\rho^2$, with $m_{s,\text{eff}}^2 = m_s^2 + \kappa\phi_0 + \frac{\lambda}{2}\phi_0^2 + g_s^2(d\rho_s^0/dM^*)$. From Eq. (11) we get the following dispersion relation

$$\left[1 + C_A^{ee}L(s_e)\right][1 + L(s_p)F^{pp} + L(s_n)F^{nn} + L(s_p)L(s_n)(F^{pp}F^{nn} - F^{pn}F^{np})] - C_A^{ep}C_A^{pe}L(s_e)L(s_p)[1 + L(s_n)F^{nn}] = 0, \quad (13)$$

with $F^{ij} = (C_s^{ij} - C_v^{ij} - \tau_i\tau_j C_\rho^{ij})$.

At low densities, corresponding to a negative value of the compressibility, the system presents unstable modes characterized by an imaginary frequency. To obtain these modes, one has to replace s with $i\beta$ in Eq. (12). In this case, the Lindhard functions become

$$L(i\beta) = 1 - \beta\tan^{-1}(1/\beta). \quad (14)$$

IV. THERMODYNAMICAL INSTABILITIES

In the present work, we have taken into account the effect of electrons on the instability zone of neutral matter. We have considered two different situations: The Coulomb interaction is switched on or switched off. We also look at two types of instabilities: Dynamical and thermodynamical instabilities. In the first case the spinodal section corresponds to the occurrence

of unstable modes, i.e., to imaginary solutions of the dispersion relations. This spinodal region thus depends on the momentum transfer k. One can then define the envelope of the spinodal region for all k as the dynamical instability region.

In the thermodynamical case, the spinodal is obtained following the prescription given in Ref. [17], which is related to the minimization of the free energy because we can consider the volume and temperature constant. This stability condition imposes that the free-energy density $\mathcal{F}$ is a convex function of the densities [17,30,31]. Because star matter should be globally uncharged only two densities are independent thermodynamical variables ρ_n and $\rho' = \rho_p = \rho_e$. In the mean-field approach the free energy is the sum of the nuclear ($\mathcal{F}_N$) and of the electron ($\mathcal{F}_e$) free energies:

$$\mathcal{F}(\rho_n, \rho') = \mathcal{F}_N(\rho_n, \rho_p = \rho') + \mathcal{F}_e(\rho_e = \rho').$$

The two densities ρ_n and ρ' are thus associated to two chemical potentials $\mu_n = \partial\mathcal{F}_N/\partial\rho_n$ and $\mu = \mu_p + \mu_e$ with $\mu_p = \partial\mathcal{F}_N/\partial\rho_p$ and $\mu_e = \sqrt{m_e^2 + P_{Fe}^2}$. In fact, if the electrons compensate for the protons charge, we have $\rho_p = P_{Fp}^3/3\pi^2 = \rho_e = P_{Fe}^3/3\pi^2$, which implies that $P_{Fp} = P_{Fe}$. The free energy curvature matrix is then

$$\mathcal{C} = \begin{pmatrix} \dfrac{\partial\mu_n}{\partial\rho_n} & \dfrac{\partial\mu_n}{\partial\rho_p} \\ \dfrac{\partial\mu_p}{\partial\rho_n} & \dfrac{\partial\mu_p}{\partial\rho_p} + \dfrac{\partial\mu_e}{\partial\rho_e} \end{pmatrix}, \tag{15}$$

and the stability condition requires that this matrix is positive. This is equivalent to imposing

$$\mathrm{Tr}(\mathcal{C}) > 0, \tag{16}$$

$$\mathrm{Det}(\mathcal{C}) > 0. \tag{17}$$

The eigenvalues of the stability matrix are given by

$$\lambda_\pm = \tfrac{1}{2}[\mathrm{Tr}(\mathcal{C}) \pm \sqrt{\mathrm{Tr}(\mathcal{C})^2 - 4\mathrm{Det}(\mathcal{C})}], \tag{18}$$

and the eigenvectors $\boldsymbol{\delta\rho}^\pm$ by

$$\frac{\delta\rho^\pm}{\delta\rho_n^\pm} = \frac{\lambda^\pm - \dfrac{\partial\mu_n}{\partial\rho_n}}{\dfrac{\partial\mu_n}{\partial\rho_p}}.$$

The stability condition requires that the two eigenvalues are positive. When one curvature turns negative the system is thermodynamically unstable and can decrease its free energy by going in the instability direction. In the nuclear case, the largest eigenvalue is always positive but the other may become negative defining the thermodynamical spinodal.

V. NUMERICAL RESULTS AND DISCUSSIONS

In Fig. 1 we plot the instability zones for different situations: Standard nuclear matter with no inclusion of electrons (light gray region), thermodynamical spinodal with electrons (dark gray region), and the envelope of the dynamical instability regions for a finite k when the Coulomb interaction is included (medium gray region). In this last case, we plot the spinodal

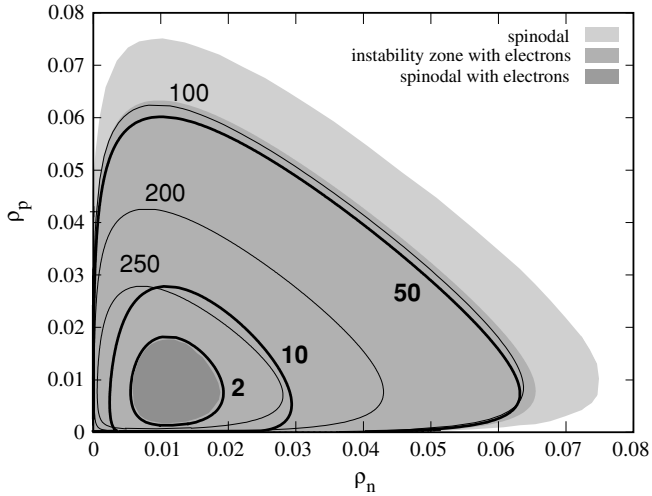

FIG. 1. The thermodynamical instability region without (light gray) and with (dark gray) electrons is represented. The envelope of the dynamical instability region is defined by the medium gray region. Dynamical spinodal sections for different momenta transfer k are represented by a thick (thin) line for $k \lesssim 80\,\mathrm{MeV}/c$ ($k > 80\,\mathrm{MeV}/c$). Momenta transfers are given in MeV/nucleon.

for different values of the momentum transfer k (thick and thin lines). The limiting envelope corresponds to momenta $\sim$70$-$80 MeV/nucleon.

Focusing first on the thermodynamical instabilities, Fig. 1 shows that the presence of the electrons contributes to reduce the size of the instability region. The strong incompressibility of the degenerated relativistic electron gas is stabilizing the nuclear instability against density fluctuations because at the thermodynamical limit the proton and electron densities should be exactly equal to ensure electric neutrality. This cancellation is so strong that only a small instability region is left. However, the presence of an unstable region in this case is certainly model dependent. Although the TM1 parametrization of NLWM [32] also has a similar unstable region, in the mean-field relativistic model with density-dependent coupling parameters [33] there is no thermodynamical unstable region once electrons are included.

Considering finite k density modulation, one is not forced to keep the electroneutrality locally so that electron and protons can fluctuate independently leading to a larger instability region. However, the inclusion of the proton-electron infinite range coupling forces the proton and electron fluctuations to be in phase at the infinite wavelength limit. The $k = 0$ limit of the dynamical instability thus leads to the small thermodynamical instability region. One observes that the influence of the electrons decreases, as k increases up to $k \lesssim$ 70$-$80 MeV/nucleon (thick lines). This is expected because the Coulomb contribution varies with the inverse of the momentum square, becoming weaker at large k. For higher values of k, this effect becomes negligible and we recover the behavior already observed in Ref. [22], i.e., the instability region decreases with the increase in the momentum transfer (thin lines). This is in fact coming from the finite range of the nuclear interaction that reduces the binding of the matter

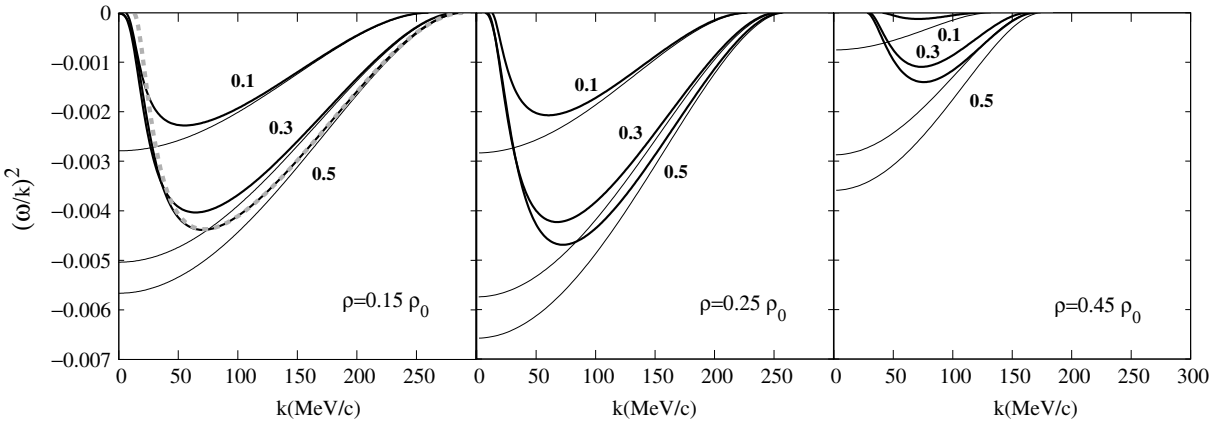

FIG. 2. The ratios $(\omega/k)^2$ are given for $y_p = 0.1, 0.3,$ and 0.5 and three densities ($0.15\rho_0$, $0.25\rho_0$, $0.45\rho_0$). Thick (thin) lines correspond to results with (without) electrons. The dotted gray curve in the first graph, $\rho = 0.15\rho_0$, was obtained considering the electrons blocked, $\delta\rho_e = 0$.

with a k^2 term and leads to a reduction of the spinodal region at large k. It should be noticed that although the spinodal region is strongly asymmetric at small k because of the electron stabilizing effect, it becomes almost symmetric at large k with the reduction of the coupling with electrons.

In Fig. 2 we plot the ratio $(\omega/k)^2$ for $y_p = 0.1$, 0.3, and 0.5 and three different densities representative of three different regions of the instability zone: $0.45\,\rho_0$ is close to the borderline, $0.15\,\rho_0$ tests the small k region, and $0.25\,\rho_0$ is a standard middle instability zone value. For comparison we present both the nuclear matter results (thin line) and the electron-neutralized nuclear matter results (thick line). The nuclear matter case presents the standard phenomenology: At low k, ω/k converges toward a well-defined imaginary velocity of sound, whereas at large k the finite range of the nuclear force reduces the instability. The introduction of electrons and Coulomb force has several consequences. As already seen, for small k the unstable mode disappears, except for the lowest density value if $y_p > 0.22$. However, even for this density the behavior of the ratio ω/k differs from the nonelectron case: Although in the last case we get (imaginary) sound velocities for $k = 0$ corresponding to a linear dependence of ω on k, in the first case $\omega(k)$ has a more complex k dependence and $(\omega/k)^2$ converges toward a very small value $(\omega/k)^2 \sim 10^{-6} - 10^{-5}$. This quenching of the instability is directly due to the $1/k^2$ divergence of the Coulomb energy. If the electrons would be blocked this divergence would directly lead to a systematic suppression of the instability at low k. This is clearly shown in Fig. 2 by the dotted curve plotted for $\rho = 0.15\rho_0$ and obtained with $y_p = 0.5$. The observed region of densities in which the instability survives even at the thermodynamical limit $k \longrightarrow 0$ shows that the nuclear instability is strong enough to drag the electron. Because of the high electron compressibility this is possible only at low electron (and so proton) density and small isospin asymmetry. In the large k limit the effect of the Coulomb interaction goes to zero so that the instability converges toward the nuclear matter results. The quenching of high k instability is thus due to the finite range of the nuclear attractive force.

Being quenched at low and high k, the neutralized nuclear matter dispersion relation thus presents a maximum. For a given value of the total density, the most unstable mode corresponding to the largest value of ω occurs at a value of k that decreases only slightly with the proton fraction y_p, namely $\sim$10% from $y_p = 0.5$ to $y_p = 0.1$. For $\rho = 0.15\rho_0$, $0.25\rho_0$, $0.45\rho_0$, we get this maximum respectively at $k \sim 170$, 150, and 100 MeV/nucleon.

It is also instructive to look at the instability direction to understand the nature of unstable modes. In Fig. 3 the ratios

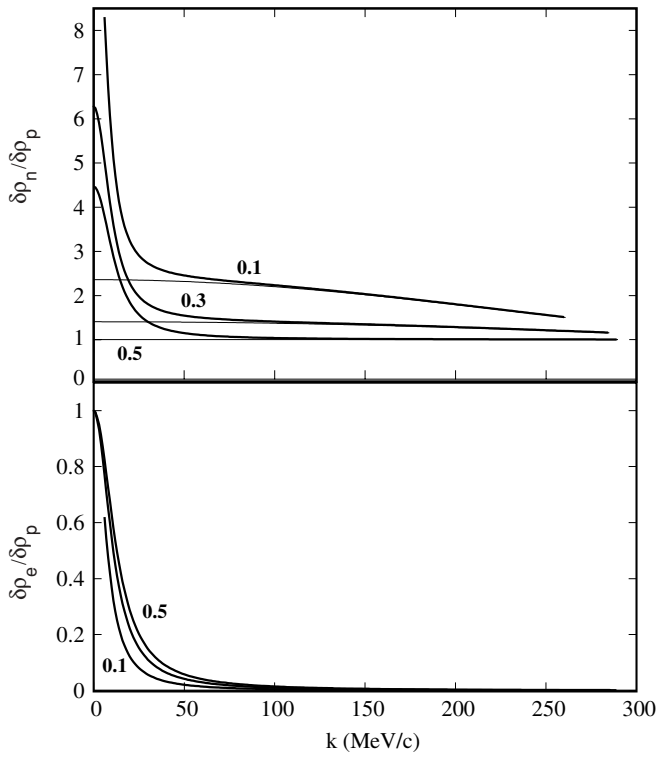

FIG. 3. The ratios $d\rho_n/d\rho_p$ (upper figure) and $d\rho_e/d\rho_p$ (lower figure) for $y_p = 0.1, 0.3,$ and 0.5 and $\rho = 0.15\rho_0$. Thick (thin) lines correspond to results with (without) electrons.

$\delta\rho_n/\delta\rho_p$ and $\delta\rho_e/\delta\rho_p$ are shown for $\rho = 0.15\rho_0$ and different proton fractions, symmetric matter ($y_p = 0.5$) and neutron-rich matter ($y_p = 0.3$ and $y_p = 0.1$), including (thick lines) and not including (thin lines) the Coulomb interaction.

Let us first focus on $\delta\rho_n/\delta\rho_p$ (top part of the figure). For comparison the proton fraction $y_p = 0.3$ corresponds to a ratio $\rho_n/\rho_p = 2.333$ and $y_p = 0.1$ to $\rho_n/\rho_p = 9$. The asymmetric nuclear matter results (thin lines) are almost independent of k. They correspond to values lower then the actual ratio ρ_n/ρ_p (see also Ref. [22]). Therefore, unstable modes produce more symmetric dense matter (liquid) and more asymmetric gas. This corresponds to the distillation effect: Nuclear matter in the denser phase prefers to be closer to symmetric matter. This effect is very clear in a mean-field calculation of droplets formation in asymmetric nuclear matter [19].

Including Coulomb field changes this picture at low k and the ratio $\delta\rho_n/\delta\rho_p$ may get larger than ρ_n/ρ_p: Proton motion becomes blocked by the Coulomb repulsion and increasing proton fraction in the dense phase would cost more energy than the gain coming from the nuclear symmetry energy. This effect is so strong that the direction of the instability crosses the constant proton fraction line, inverting the neutron distillation phenomenon. When $\delta\rho_n/\delta\rho_p$ becomes larger then the actual asymmetry ρ_n/ρ_p the dense phase (clusters and nuclei) becomes even more exotic than the initial matter while the gas phase is enriched in protons. However, this antidistillation effect occurs at k that are smaller than the k values of the most unstable modes. Therefore, one may expect that the dominating partitions will not show such an abnormal isospin distillation. Only large clusters are expected to present this exoticity enhancement. The actual effect on the gas and on the cluster-size dependence of the proton fraction requires a much more elaborated treatment and remains an open question.

Let us now turn to the electron content of the unstable modes (bottom part of Fig. 3). To reduce the Coulomb energy the electrons are forced to move in phase with the protons; however, because of their relativistic and fermionic nature this motion has a strong kinetic price. Only at $k = 0$ protons and electrons strictly move in phase to ensure the charge neutrality as imposed by this thermodynamical limit: For $k = 0$, $\delta\rho_e/\delta\rho_p$ is 1. This electronic polarization occurs only for small k values and tries to compensate the increase of the Coulomb energy enlarging the instability zone.

Next we discuss the density dependence of the unstable mode. We can fix the proton density, $\rho_p = 0.01$ fm^{-3} and vary the neutron density, i.e., we move on a line parallel to the ρ_n axis of Fig. 1. In Fig. 4 we give both ratios $(\omega/k)^2$ and $\delta\rho_n/\delta\rho_p$ for two values of k, 5 and 100 MeV/nucleon. The smallest value, 5 MeV/nucleon, explores the small thermodynamical unstable region between 0.005 fm$^{-3} < \rho_n < 0.02$ fm^{-3} or total density 0.015 fm$^{-3} < \rho_n < 0.03$ fm^{-3}. We point out that values of $\rho_n < 0.01$ fm^{-3} correspond to proton-rich matter and otherwise neutron-rich matter. As discussed before the effect of the Coulomb interaction and of electrons is small for $k = 100$ MeV/nucleon. The isospin content $\delta\rho_n/\delta\rho_p$ and the actual frequency are modified by less then 10% by the electromagnetic interaction. The behavior $\delta\rho_n/\delta\rho_p > \rho_n/\rho_p$ for proton-rich matter and $\delta\rho_n/\delta\rho_p < \rho_n/\rho_p$ for neutron-rich matter show clearly the preference of the system for symmetric nuclear matter. This is the usual isospin distillation. A quite different situation occurs for $k = 5$ MeV/nucleon: The instability is strongly reduced and $\delta\rho_n/\delta\rho_p$ is always larger than ρ_n/ρ_p. Even for the most neutron-rich unstable matter $\delta\rho_n/\delta\rho_p$ is still $2\rho_n/\rho_p$. This antidistillation phenomenon seems to be a general characteristic of long wavelength (small k) instabilities that would lead to large clusters with enhanced exoticity.

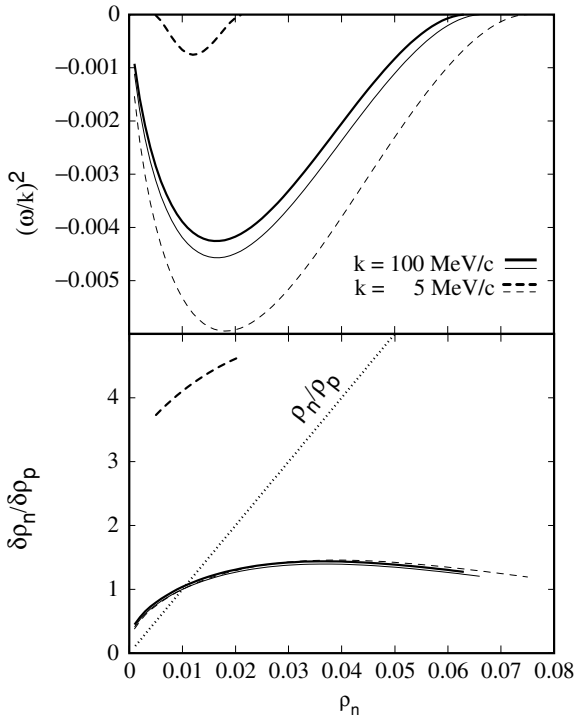

FIG. 4. The ratios $(\omega/k)^2$ (upper figure) and $d\rho_n/d\rho_p$ (lower figure) versus the neutron density for $\rho_p = 0.01$ fm^{-3} and two different momenta $k = 5$ and 100 MeV/nucleon. Thick (thin) lines correspond to results with (without) electrons. The dotted line in the lower figure represents the ratio ρ_n/ρ_p.

VI. CONCLUSIONS

In the present work, we have looked at dynamical and thermodynamical instabilities of nuclear neutral matter, which is of interest for the study of neutron stars and supernovae. In particular, we have studied the importance of including the Coulomb interaction on the instability region and the actual role of the degenerated gas of electrons. The calculations were performed within a relativistic mean-field approach to nuclear matter, namely the NL3 parametrization of the NLWM, but we believe that the main conclusions with respect to the dynamical instabilities do not depend on the model. It was shown that, at the mean-field level, the instability region is drastically reduced for neutral matter with respect to nuclear matter with the Coulomb interaction switched off. Depending on the force, at the thermodynamical limit the spinodal region may also disappear because of the strong incompressibility of the electron gas. However, this reduction is small if the Coulomb

interaction is properly taken into account within a dynamical calculation looking at finite k instabilities. Structures with a size $\sim$7 fm, corresponding to momenta 70–80 MeV/nucleon, are the first to become unstable. This defines a wide instability region. Smaller structures (larger k) stabilize nuclear matter because of the finite range of the nuclear attraction as already seen in Ref. [22] and larger structures are unstable in a smaller density region because of the long range Coulomb interaction. The main effect of the Coulomb interaction is to block the protons at small k increasing the neutron density fluctuations with respect to proton density ones. This may be so dramatic that even in neutron-rich matter fluctuations tend to increase asymmetry of the dense phase contrary to what generally is accepted as the distillation effect. However, we have shown that the most unstable mode depends only slightly on the isospin asymmetry and on the density, and it corresponds to structures of $\sim$7–10 fm. If we consider structures of such a size ($\sim$10 fm) the associated k are large enough to not introduce large differences on the results because of the Coulomb interaction. For such characteristic length the only effect is a small reduction of the instability and so of the borderline of the unstable region.

The calculation presented includes the electron dynamics. Only for large wavelengths is the gain in Coulomb energy sufficient to compensate for the loss because of the high-electron Fermi energy, and electrons start to move in phase with the protons. For the considered nuclear interaction this phenomenon even leads to the survival of an instability at the thermodynamical limit $k \to 0$.

The present results will mainly have implications in astrophysical objects, because we are dealing with neutral matter, namely in transport properties. In particular it is known that neutrino interactions are crucial in the dynamics of the core-collapse supernovae because they carry most of the energy away. In Ref. [34] it was shown that coherent neutrino scattering from nonuniform hadron-quark matter or hadron matter with and without kaon condensed phase would greatly reduce the neutrino mean-free path. A similar effect at low densities could allow enough energy transfer to revive the supernova shock. Our work focuses on the low-density regions.

Recent semiclassical simulations of the linear response of nuclear nonhomogeneous matter at low densities, the so-called nuclear pasta, to neutrinos in Ref. [35] have shown that coherence effects reduce the mean free path of neutrinos. In these simulations electrons are not modeled explicitly, but their effect is included through a modified Coulomb interaction between the protons through a screening length (taken equal to 10 fm). Neutrinos will lose energy by exciting collective nuclear modes or plasmon modes. As stated above, our calculation shows that the behavior of the electrons depends on the wavelength of the perturbation.

In Ref. [36] low-energy nuclear collective excitations of Wigner-Seitz cells containing nuclear clusters immersed in a gas of neutrons have been obtained. However, the electron motion was not included. Including the electron contribution will likely affect the results for large clusters. We have also calculated the wavelengths corresponding to the most unstable modes that give the order of magnitude of the size of the clusters that will most probably be formed and therefore determine the neutrino wavelengths that could be most sensitive to the inhomogeneous phase. It should be noticed that the instabilities we compute are connected with the creation of inhomogeneities. The elastic scattering of neutrinos on the created clusters reduces their mean-free path.

All the calculations were done at $T = 0$ MeV: The effect of dynamical instabilities, including the Coulomb field, should also be investigated at finite T. Understanding the mixed phase of neutral matter at finite temperature is important to determine the behavior of neutrinos emitted in a supernova explosion.

ACKNOWLEDGMENTS

This work was partially supported by Capes (Brazil) under process BEX 1681/04-4, CAPES(Brazil)/GRICES (Portugal) under project 100/03 and FEDER/FCT (Portugal) under the project POCTI/FP/FNU/50326/2003. D.P.M. thanks the friendly atmosphere at the Research Center for Theoretical Astrophysics in the Sydney University, where this work was partially done.

[1] J. M. Lattimer, Annu. Rev. Nucl. Part. Sci. **31**, 337 (1981).
[2] B. Link, R. I. Epstein, and G. Baym, Astrophys. J. **403**, 285 (1993).
[3] S. Nishizaki, T. Takatsuka, and J. Hiura, Prog. Theor. Phys. **92**, 93 (1994).
[4] C. J. Pethick, D. G. Ravenhall, and C. P. Lorenz, Nucl. Phys. **A584**, 675 (1995).
[5] T. Alm *et al*., Nucl. Phys. **A604**, 491 (1996).
[6] B. Malakar and S. Sarkar, Prog. Theor. Phys. **98**, 601 (1997).
[7] H. Huber *et al*., Int. J. Mod. Phys. E **7**, 301 (1998).
[8] K. Strobel, F. Weber, and M. K. Weigel, Z. Naturforsch. A **54a**, 83 (1999).
[9] F. Douchin and P. Haensel, Phys. Lett. **B485**, 107 (2000).
[10] N. K. Glendenning, Phys. Rep. **342**, 393 (2001).
[11] C. Ishizuka, A. Ohnishi, and K. Sumiyoshi, Prog. Theor. Phys. suppl. **146**, 373 (2002).
[12] P. Magierski and P. H. Heenen, Phys. Rev. C **65**, 045804 (2002).
[13] G. Watanabe, K. Sato, K. Yasuoka, and T. Ebisuzaki, Phys. Rev. C **69**, 055805 (2004).
[14] C. J. Horowitz, M. A. Perez-Garcia, and J. Piekarewicz, Phys. Rev. C **69**, 045804 (2004).
[15] Ph. Chomaz and F. Gulminelli, Phys. Lett. **B447**, 221 (1999); H. S. Xu *et al*., Phys. Rev. Lett. **85**, 716 (2000).
[16] Ph. Chomaz, Nucl. Phys. **A685**, 274c (2001).
[17] J. Margueron and P. Chomaz, Phys. Rev. C **67**, 041602(R) (2003); P. Chomaz, M. Colonna, and J. Randrup, Phys. Rep. **389**, 263 (2004).
[18] S. S. Avancini, L. Brito, D. P. Menezes, and C. Providência, Phys. Rev. C **70**, 015203 (2004).
[19] D. P. Menezes and C. Providência, Phys. Rev. C **64**, 044306 (2001); C. Providência, D. P. Menezes, and L. Brito, Nucl. Phys.

A703, 573 (2002); D. P. Menezes and C. Providência, Phys. Rev. C **60**, 024313 (1999); B. Jacquot, S. Ayik, Ph. Chomaz, and M. Colonna, Phys. Lett. **B383**, 247 (1996).
[20] Ph. Chomaz, F. Gulminelli, C. Ducoin, P. Napolitani, and K. H. O. Hasnaoui, submitted; astro-ph/0507633.
[21] R. F. Sawyer, Phys. Rev. D **11**, 2740 (1975); N. Iwamoto and C. J. Pethick, *ibid*. **25**, 313 (1982).
[22] S. Avancini, L. Brito, D. P. Menezes, and C. Providência, Phys. Rev. C **71**, 044323 (2005).
[23] G. A. Lalazissis, J. König, and P. Ring, Phys. Rev. C **55**, 540 (1997).
[24] L. D. Landau and E. M. Lifshitz, *The Classical Theory of Fields* (Addison-Wesley, Reading, MA, 1951), p. 10.
[25] M. Nielsen and J. da Providência, Phys. Rev. C **40**, 2377 (1989).
[26] M. Nielsen, C. Providência, and J. da Providência, Phys. Rev. C **44**, 209 (1991); M. Nielsen, C. da Providência, J. da Providência, and Wang-Ru Lin, Mod. Phys. Lett. A **10**, 919 (1994); M. Nielsen, C. Providência, and J. da Providência, Phys. Rev. C **47**, 200 (1993).
[27] K. Lim and C. J. Horowitz, Nucl. Phys. **501**, 729 (1989).
[28] S. Reddy, M. Prakash, and J. M. Lattimer, Phys. Rev. D **58**, 013009 (1998); S. Reddy, M. Prakash, J. M. Lattimer, and J. A. Pons, Phys. Rev. C **59**, 2888 (1999).
[29] K. Saito, T. Maruyama, and K. Soutome, Phys. Rev. C **40**, 407 (1989).
[30] H. Müller and B. D. Serot, Phys. Rev. C **52**, 2072 (1995).
[31] V. Baran, M. Colonna, M. Di Toro, and A. B. Larionov, Nucl. Phys. **A632**, 287 (1998).
[32] K. Sumiyoshi, H. Kuwabara, and H. Toki, Nucl. Phys. **A581**, 725 (1995).
[33] S. Typel and H. H. Wolter, Nucl. Phys. **A656**, 331 (1999).
[34] S. Reddy, G. Bertsch, and M. P. Prakash, Phys. Lett. **B475**, 1 (2000).
[35] C. J. Horowitz, M. A. Perez-Garcia, D. K. Berry, and J. Piekarewicz, Phys. Rev. C **72**, 035801 (2005); C. J. Horowitz, M. A. Perez-Garcia, J. Carriere, D. K. Berry, and J. Piekarewicz, *ibid*. **70**, 065806 (2004); C. J. Horowitz, M. A. Perez-Garcia, and J. Piekarewicz, *ibid*. **69**, 045804 (2004).
[36] E. Khan, N. Sandulescu, and Nguyen Van Giai, Phys. Rev. C **71**, 042801(R) (2005).